

Application of mid-infrared free-electron laser tuned to amide bands for dissociation of aggregate structure of protein

Takayasu Kawasaki,^{a,*} Toyonari Yaji,^b Toshiaki Ohta^b and Koichi Tsukiyama^a

Received 10 June 2015

Accepted 2 November 2015

Edited by M. Yabashi, RIKEN SPring-8 Center, Japan

Keywords: amide band; keratin aggregate; mid-infrared free-electron laser; protein aggregate.

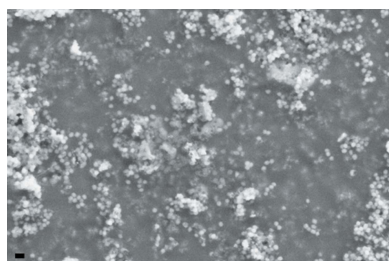
^aIR Free Electron Laser Research Center, Research Institute for Science and Technology, Organization for Research Advancement, Tokyo University of Science, 2641 Yamazaki, Noda, Chiba 278-8510, Japan, and ^bSR Center, Research Organization of Science and Technology, Ritsumeikan University, 1-1-1 Noji-Higasi, Kusatsu, Shiga 525-8577, Japan.

*Correspondence e-mail: kawasaki@rs.tus.ac.jp

A mid-infrared free-electron laser (FEL) is a linearly polarized, high-peak powered pulse laser with tunable wavelength within the mid-infrared absorption region. It was recently found that pathogenic amyloid fibrils could be partially dissociated to the monomer form by the irradiation of the FEL targeting the amide I band (C=O stretching vibration), amide II band (N–H bending vibration) and amide III band (C–N stretching vibration). In this study, the irradiation effect of the FEL on keratin aggregate was tested as another model to demonstrate an applicability of the FEL for dissociation of protein aggregates. Synchrotron radiation infrared microscopy analysis showed that the α -helix content in the aggregate structure decreased to almost the same level as that in the monomer state after FEL irradiation tuned to 6.06 μm (amide I band). Both irradiations at 6.51 μm (amide II band) and 8.06 μm (amide III band) also decreased the content of the aggregate but to a lesser extent than for the irradiation at the amide I band. On the contrary, the irradiation tuned to 5.6 μm (non-absorbance region) changed little the secondary structure of the aggregate. Scanning-electron microscopy observation at the submicrometer order showed that the angular solid of the aggregate was converted to non-ordered fragments by the irradiation at each amide band, while the aggregate was hardly deformed by the irradiation at 5.6 μm . These results demonstrate that the amide-specific irradiation by the FEL was effective for dissociation of the protein aggregate to the monomer form.

1. Introduction

A mid-infrared free-electron laser (FEL) employs synchrotron radiation as a light source for lasing and provides a specific pulse profile with complete linear polarization, frequency tunability within the mid-infrared region, and high photon density. The FEL has been used for spectroscopic studies of molecules, thermodynamic analyses of biomolecules, and surgical ablation of pathological tissues (Austin *et al.*, 2005; Dunbar *et al.*, 2011; Edwards & Hutson, 2003). In particular, the laser ablation process is effective in removal of tumor tissues in laser-mediated therapeutic strategy, under which the tissue absorbs many photons of the laser beam and more than 60% of water is vaporized from the internal space of the tissue. This ablation process can induce dynamic structural changes of protein matrices such as collagen protein (Anderson & Parrish, 1983; Xiao *et al.*, 2008). We are attempting to apply the FEL at Tokyo University of Science (FEL-TUS) to biomedical fields as well as basic physical chemistry and to supply the beamline for related researchers all over the world (Miyamoto *et al.*, 2011; Nomaru *et al.*, 2000).



The oscillation wavelength range available at FEL-TUS is from 5.0 μm to 14 μm , which contains the amide I band (C=O stretching vibration at 6.0–6.2 μm), the amide II band (N–H bending vibration at 6.4–6.6 μm) and the amide III band (C–N stretching vibration at 7.7–7.9 μm) (Bandekar, 1992). Recently, we found that the FEL tuned to these amide bands can promote dissociation of amyloid fibrils of lysozyme and insulin peptide to their monomer structures (Kawasaki *et al.*, 2012, 2014). Amyloid fibrils are a variety of aggregate structures of proteins, and the aggregation process often causes several neurodegenerative diseases and amyloidosis (Sipe *et al.*, 2014). Although disaggregation of these aggregates is expected to lead to amelioration of pathologies, the aggregated structures are commonly robust under physiological conditions, and it is difficult to dissolve the aggregate forms unless detergents or organic solvents are used which are often toxic for the human body. For the mechanism of dissociation of amyloid fibrils under the FEL irradiation condition, it can be proposed that non-covalent bonds such as hydrogen bonds between β -sheets are disrupted by the FEL energy absorption at the amide bands (Kawasaki *et al.*, 2012). The method using the FEL is expected to be novel and valuable for decreasing such a pathological protein aggregate instead of traditional biochemical reagents. In this study, we targeted another aggregate, keratin aggregate, in order to test whether the FEL would be valid for dissociation of other protein aggregates than amyloid fibrils.

Keratin is a major structural component of cytoskeleton in both hair and skin tissues, and is involved in the formation of cuticle structures, which is well known in the fields of dermatology and plastic surgery (Chamcheu *et al.*, 2011; Irvine & McLean, 1999). Keratin tends to form non-covalent assembly during aging similarly to the amyloid peptides, and the aggregation process causes hair damage and several skin diseases. While amyloid peptide is small in molecular size, 1–10 kDa, in general, keratin is a comparatively large protein, approximately 50 kDa (Marchuk *et al.*, 1985). It is interesting how an aggregate structure of such a large-sized protein should be dissociated to the monomer form by the action of the FEL. We set up the FEL irradiation condition to be the same as the case of amyloid fibrils, and analyzed the secondary structural and morphological changes of the keratin aggregate after the FEL irradiation tuned to the amide bands.

2. Materials and methods

2.1. Materials

The reagents were purchased as special-grade chemicals. Dimethyl sulfoxide (DMSO) and phosphate buffered saline (PBS; 10 mM) were purchased from Wako Pure Chemical Industries (Osaka, Japan). Keratin was purchased from Nacalai Tesque (Kyoto, Japan).

2.2. FEL-generation system

The experimental setup of FEL-TUS was described in detail previously (Kawasaki *et al.*, 2012, 2014). Briefly, the FEL is

generated using synchrotron radiation (SR) as a seed with a variable wavelength in the mid-infrared region (5.0–14 μm ; 714–2000 cm^{-1}). The electron beam was generated by a high radio-frequency (RF) electron gun (2856 MHz), and injected into an undulator through an α -magnet and a linear accelerator. The maximum acceleration energy is 40 MeV, and the electron beam is forced to oscillate in the undulator to produce SR. SR is amplified between a pair of mirrors positioned at both sides of the undulator through the interaction with the electron beam, producing coherent laser light (FEL). The wavelength of the FEL can be tunable by adjusting the space interval of the undulator, and the half-width of the waveform of the FEL was usually 0.1–0.2 μm at most wavelengths. The time structure of the FEL is composed of macro- and micro-pulses. The full width at half-maximum (FWHM) of the micro-pulse is 1–2 ps and the interval of the consecutive micro-pulses is 350 ps. A pulse train of the micro-pulses forms a single macro-pulse which has a duration of 2 μs . The repetition rate of the macro-pulse is 5 Hz during operation. The pulse energy per macro-pulse was in the range 7.0–9.0 mJ, as measured using an energy meter (SOLO2, Gentec-EO Inc., Quebec, Canada). Prior to the irradiation, the FEL beam was focused almost to the whole area of the sample (~ 0.5 cm in diameter) under the guidance of a He–Ne beam. The power densities of the FEL were estimated to be 35–45 mJ cm^{-2} .

2.3. Preparation of keratin aggregate and FEL irradiation method

Keratin powder was dissolved in DMSO to 10 mg ml^{-1} , and the stock solution was diluted by four times the volume of PBS containing 2 M NaCl, and incubated at 37°C for one day. The aggregate was washed with water and mixed with water (300 μL) for the stock solution after being collected by centrifugation at 14 krpm for 10 min. For measuring the FEL transmittance, the air-dried aggregate was mixed with potassium bromide (KBr) powder, and the mixture was processed in a mini-circle plate (diameter: 0.5 cm; thickness: ~ 0.1 mm) by using a press implement (Jasco, Japan). The FEL, tuned to various wavelengths, was irradiated to the plate as describe above, and the power energy of the FEL was measured at the front and the back of the plate. For microscopic analyses of the irradiated samples, the aggregated material (30 μL) was spotted on the glass slide (for electron microscopy) or stainless-steel base (for infrared microscopy) and irradiated by the FEL at 37°C for 1 h. After the irradiation was completed, the sample was air-dried for at least 20 h at room temperature, and subjected to microscopic analyses as described below.

2.4. Synchrotron radiation infrared microscopy (SR-IRM) analysis

SR-IRM analysis was performed using the IR micro-spectroscopy beamline (SRMS, BL-15) at the SR Center of Ritsumeikan University as shown in a previous study (Yaji *et al.*, 2008). The beamline is equipped with Nicolet 6700 and Continuum XL IR microscopes (Thermo Fisher Scientific). Measurements were performed in reflection mode with a 32 \times

Cassegrain lens and a 20 $\mu\text{m} \times 20 \mu\text{m}$ aperture. Spectra were collected in the mid-IR range of 700–4000 cm^{-1} at a resolution of 4 cm^{-1} with 64 scans. Smoothing and normalization of spectra were performed in the region containing the amide bands (1000–2000 cm^{-1}) by using *Spectra Manager* software (version 2) (Jasco International, Tokyo, Japan). Secondary structure contents were estimated by measuring the peak intensity around the amide I band by using the attached protein analysis software (*IR-SSE*; JASCO), which was developed for evaluation of protein conformational changes in carcinoma tissue (Yamada *et al.*, 2002).

2.5. Scanning electron microscopy (SEM) analysis

The morphology of keratin aggregate was analyzed using an FE-SEM Supra40 scanning electron microscope (Carl Zeiss). After generating keratin aggregates as described above, the dried material on the glass slide was fixed on a sample holder using conductive copper tape and injected into the vacuum chamber. The acceleration voltage was set to 5.0 kV, and the observation was performed at an oblique position (SE2 mode).

3. Results

3.1. Wavelength-dependent absorption of FEL energy into the keratin aggregate

In order to estimate the FEL energy absorbed by the keratin aggregate, we measured the FEL transmittance at several wavelengths (Fig. 1*a*). The infrared absorption spec-

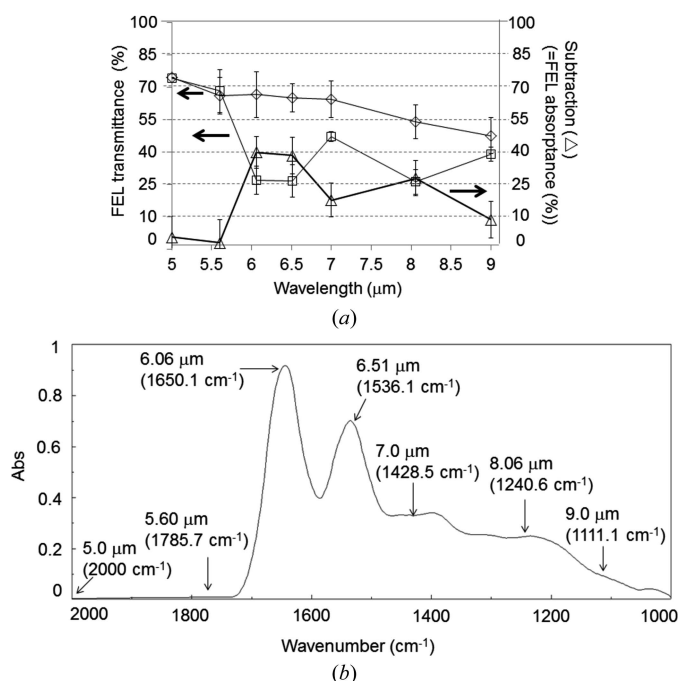


Figure 1 (a) FEL transmittance for the keratin aggregate. The bars represent the estimated error over three measurements. Diamonds: KBr only (background). Squares: KBr + keratin aggregate. Triangles: subtraction (= FEL absorbance). (b) Infrared absorption spectrum of the keratin aggregate. The spectrum was obtained by SR-infrared microscopy analysis.

Table 1 Amide frequencies (cm^{-1}) of keratin samples before and after FEL irradiation.

	Amide I	Amide II	Amide III
Monomer	1631.5	1527.3	1209.1
Aggregate	1645.0	1535.0	1234.2
FEL irradiation at 5.60 μm	1641.1	1535.0	1236.1
FEL irradiation at 6.06 μm	1635.3	1531.2	1232.2
FEL irradiation at 6.51 μm	1633.4	1529.3	1238.1
FEL irradiation at 8.06 μm	1637.2	1531.2	1222.6

trum of the keratin aggregate is shown in Fig. 1*b*). Compared with the background transmittance (diamonds), the minimum transmittance for keratin aggregate (squares) was found at 6.06 μm (amide I) and 6.51 μm (amide II), and the FEL absorbance at 8.06 μm (amide III) was less than those at the amide I and II bands, which is apparent in the subtraction (triangles). Below 5.6 μm , the FEL transmittance of keratin aggregate was almost the same as that of the background. Therefore, nearly half of the FEL energy was absorbed by the keratin aggregate at the amide I and II bands, and a little of the energy was absorbed at 5–5.6 μm . Next, the effect of the FEL energy absorption at the amide bands on dissociation of the aggregate structure of keratin was investigated.

3.2. Secondary structure analysis of the keratin aggregate using SR-IRM

SR-IRM improves the spatial resolution with a high signal-to-noise (S/N) ratio compared with IRM using a thermal radiation beam because high-power radiation can be delivered to a limited area in a small sample of several micrometers (Acerbo *et al.*, 2012). Furthermore, the SR-IRM spectrum is sensitive to the secondary structural changes of peptides, which enables us to evaluate the contents of the α -helix, β -sheet, β -turn and non-ordered structures in the peptide sample. Typical SR-IRM spectra for keratin monomer and aggregate, and the difference spectrum (aggregate minus monomer) are shown in Fig. 2*a*), and the de-convolution spectra for the monomer and aggregate are shown in Fig. 2*b*). Frequencies of the amide I, II and III bands in each spectrum are listed in Table 1. The amide I bands for the monomer and aggregate were observed at around 1631.5 cm^{-1} and around 1645.0 cm^{-1} , respectively. According to the previous study using model peptides forming the α -helix and β -sheet, the peak of amide I of the β -sheet is observed at a lower wavenumber than that of the α -helix (Bandekar, 1992). For the turn structure, the amide I is observed at a higher wavenumber than that of the α -helix (Caine *et al.*, 2012). These cited literature and the de-convolution spectrum revealed that the keratin aggregate is a mixture of α -helix, β -turn, non-ordered structures and β -sheet, while the monomer consists of mainly the β -sheet structure. Next, we selected four wavelengths, 6.06 μm (1650.1 cm^{-1}), 6.51 μm (1536.1 cm^{-1}), 8.06 μm (1240.6 cm^{-1}) and 5.60 μm (1785.7 cm^{-1}) for the irradiation experiment. The former three wavelengths correspond to amide I, II and III, respectively, and the latter is a non-absorbance wavelength. After the FEL irradiation tuned to

6.06 μm (Fig. 2c), 6.51 μm (Fig. 2d), 8.06 μm (Fig. 2e) and 5.60 μm (Fig. 2f), the peak of the amide I band of the aggregate shifted to 1635.3, 1633.4, 1637.2 and 1641.1 cm^{-1} , respectively (Table 1). These shift values were as follows: -9.7 cm^{-1} for 6.06 μm ; -11.6 cm^{-1} for 6.51 μm ; -7.8 cm^{-1} for 8.06 μm ;

-3.9 cm^{-1} for 5.6 μm . In each case, the difference spectrum (the irradiated spectrum minus the non-irradiated aggregate spectrum) is also shown (red dotted line). These results indicate that the amide I band of the aggregate shifted towards that of the monomer when the aggregate was irradiated at the

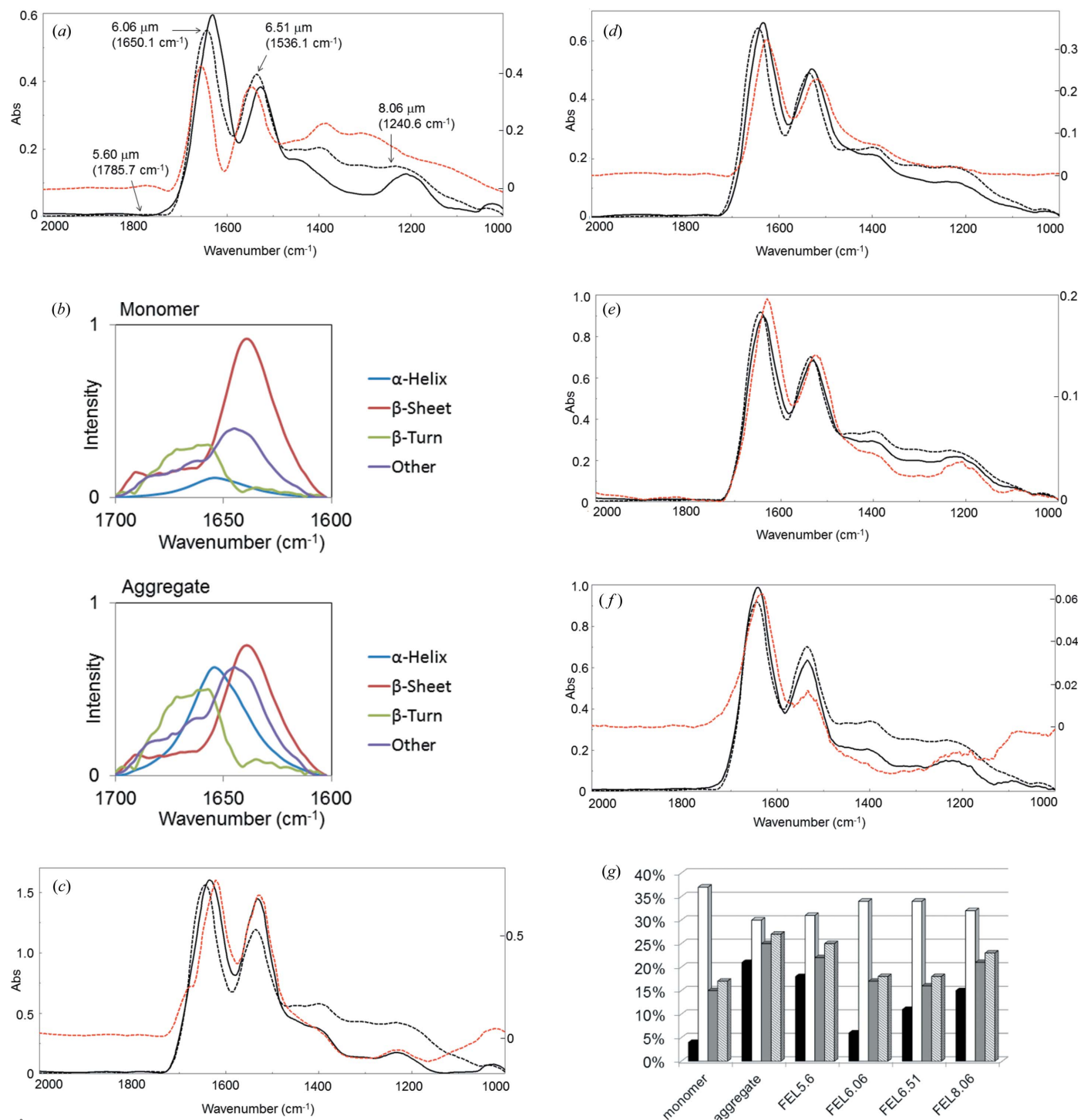


Figure 2

Synchrotron infrared microscopy analyses. (a) Reflection spectra before the FEL irradiation. Solid line: keratin monomer; dotted line: keratin aggregate; red dotted line: the difference spectrum. The scale for the difference spectrum is shown on the right-hand side of the figure. Arrows indicate FEL wavelengths for irradiation. (b) De-convolution spectra around the amide I band. (c)–(f) Reflection spectra after FEL irradiation at several wavelengths (solid lines). Dotted line: keratin aggregate; red dotted line: the difference spectrum, (c) 6.06 μm , (d) 6.51 μm , (e) 8.06 μm , (f) 5.60 μm . (g) Secondary structure analyses of the keratin monomer, keratin aggregate, keratin aggregate after the FEL irradiation at 5.60, 6.06, 6.51 and 8.06 μm . Black bar: α -helix; white bar: β -sheet; dark gray: β -turn; light gray: non-ordered structure.

amide bands, while the peak shift was smallest when the aggregate was irradiated by the FEL at 5.6 μm . The shift values of the amide II bands were as follows: -3.8 cm^{-1} for 6.06 μm ; -5.7 cm^{-1} for 6.51 μm ; -3.8 cm^{-1} for 8.06 μm ; 0 cm^{-1} for 5.6 μm . This showed that the amide II band of the aggregate also shifted near to that of the monomer when the aggregate was irradiated by the FEL at the amide bands except for 5.6 μm . On the other hand, the interpretation of the peak shifts of amide III was difficult because it was not similar to the cases of amide I and II. Although the amide III band around 1200 cm^{-1} is also known to influence the secondary conformation of peptides, its peak intensity in the aggregate was too low to analyze the conformation of keratin in this study. Next, the secondary structure content in each spectrum was evaluated by measuring the peak intensity around the amide I band (Fig. 2g), since the amide I band was most sensitively influenced by the FEL irradiation. In the aggregated form, the contents of the α -helix, β -turn and non-ordered structures were much higher than those in the monomer state, while that of the β -sheet was lower. After the FEL irradiation at 6.06 μm , the former three contents decreased to near those of the monomer while that of the β -sheet increased. Similar conformational changes were also apparent at 6.51 μm , although the three kinds of contents (α -helix, β -turn and non-ordered structures) decreased modestly after irradiation at 8.06 μm . According to expectation, a small change of these contents was recognized at 5.60 μm . It should be emphasized that 6.06 μm seemed to be the most efficient wavelength for converting the aggregate structure to the monomer state.

3.3. Morphological change of keratin aggregate after FEL irradiation

To confirm the effect of the FEL on dissociation of the keratin aggregate, we analyzed the morphological change of

the aggregate structure using SEM. The SEM image of the keratin monomer before aggregation showed many particles with approximately 100 nm diameter (Fig. 3a). After aggregation, the assembly of these particles was converted to a large-sized solid, which may be an aggregated structure of keratin (Fig. 3b). Irradiation by FEL at 6.06 μm changed the angular solid to a non-ordered assembly consisting of a number of small particles (Fig. 3c). Irradiation at 6.51 μm changed the aggregate solid to short fragments of several hundred nanometers in length (Fig. 3d). At 8.06 μm , the aggregate solid was deformed into a non-ordered structure (Fig. 3e). On the contrary, at 5.6 μm , the aggregate solid apparently remained, although the angular surface changed to a smooth surface (Fig. 3f). These observations morphologically demonstrated that the aggregate structure was dissociated by the FEL irradiation at the amide bands (I, II and III).

4. Discussion

Protein aggregation processes often cause remarkable reduction of the functional activity of the protein. In the case of keratin, the aggregation process often induces rough skin and hair damages during aging. Keratin aggregation is known to be associated with some skin diseases, and several solution strategies have been studied for reduction of the aggregated proteins from normal tissues using biological substances such as chaperone molecules (Chamcheu *et al.*, 2011). In dermatology and plastic surgery, laser-mediated therapies are well established, and skin treatment using microscopic irradiation techniques has been developed (Anderson & Parrish, 1983; Manstein *et al.*, 2004). It can be expected that co-use of the biochemical method using biological substances together with the engineering approach using laser devices will become a powerful therapeutic strategy for treatment of disease. In our

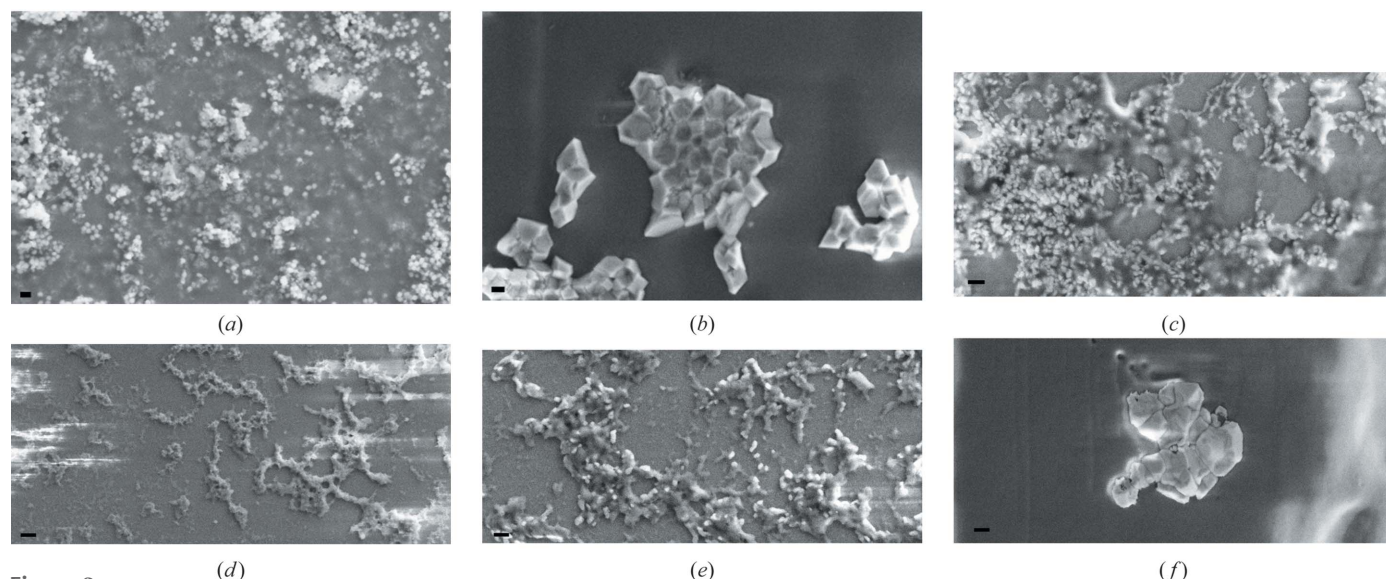


Figure 3 Structure of the keratin sample imaged with scanning electron microscopy; (a) keratin monomer, (b) keratin aggregate, (c)–(f) keratin aggregates after the FEL irradiation at several wavelengths: (c) 6.06 μm , (d) 6.51 μm , (e) 8.06 μm and (f) 5.60 μm . Scale bar: 200 nm.

previous study, we applied the FEL-TUS to dissociate amyloid aggregates to the monomer form and observed that FEL irradiation markedly affected the β -sheet content of the fibril structure (Kawasaki *et al.*, 2012, 2014). In the case of lysozyme fibrils, the resonant excitation at amide bands (I, II and III) by FEL was found to be effective for refolding the enzyme. Similarly, a dissociation effect by the FEL targeting the amide bands was observed for the keratin. Protein aggregate structure, in general, is formed commonly by non-covalent bonds such as hydrogen bonds and ionic bonds between peptide backbones, and the aggregate structure such as amyloid fibrils can be melted by external heating at over 80°C (Morel *et al.*, 2010). On the contrary, we kept the sample on a hot plate at 37°C, and the temperature on the sample increased little during the FEL irradiation in this study. According to the paper describing laser ablation of tissue by using the FEL tuned to the 6 μ m range, thermal diffusion from protein matrices to surrounding water molecules can occur within a 10–100 ns time scale after the irradiation (Hutson *et al.*, 2002). The interval and FWHM of a micro-pulse of the FEL is 350 ps and 2 ps, respectively, and so successive resonant excitation at the amide bands by micro-pulse irradiation of the FEL may satisfy the thermal confinement condition. It can be considered that this energy accumulation at the amide bands can drive the dissociation of the aggregate structure of protein to the monomer form. Furthermore, in tissue ablation with the FEL, vaporization of water is also suggested to be extremely promoted by the laser irradiation in surgery (Xiao *et al.*, 2008). In such cases, collagen protein is often denatured during the ablation process. It can be estimated that the dissociation of keratin aggregate by the FEL may proceed under the similar mechanism with the case of the conformational change of the collagen protein in ablation: FEL irradiation at the amide absorption bands heats the aggregate and surrounding water, which drives dissociation of the aggregate to the monomer form.

It can be inferred that pathological protein aggregates can be reduced by using the FEL irradiation method as described in this study. This method is as yet limited to be used for *in vitro* experiments, although the method provides specific reduction of the aggregate form to produce a non-aggregate state. For *in vivo* application of this method, examination of the irradiation conditions under which normal tissues are not damaged may be required in order to develop a more practical clinical laser device, and this project is now under planning in our laboratory.

5. Conclusion

Dissociation of the aggregate structure of keratin protein could be promoted by mid-IR FEL irradiation tuned to the amide bands. In particular, the FEL tuned to the amide I band

was most effective for reduction of the α -helix-rich aggregate structure of keratin. Together with previous results on amyloid fibrils, the mid-IR FEL is expected to be useful for dissolving the aggregate structures of proteins to their monomer forms.

Acknowledgements

We thank Dr Takayuki Imai (FEL TUS), Mr Tetsuo Morotomi and Mr Keiichi Hisazumi (Mitsubishi Electric System & Service Co. Ltd) for operating the FEL instrument. This work was supported in part by the Open Advanced Research Facilities Initiative and Photon Beam Platform Project of the Ministry of Education, Culture, Sport, Science and Technology, Japan.

References

- Acerbo, A. S., Carr, G. L., Judex, S. & Miller, L. M. (2012). *Anal. Chem.* **84**, 3607–3613.
- Anderson, R. R. & Parrish, J. A. (1983). *Science*, **220**, 524–527.
- Austin, R. H., Xie, A., van der Meer, L., Redlich, B., Lindgård, P. A., Frauenfelder, H. & Fu, D. (2005). *Phys. Rev. Lett.* **94**, 128101.
- Bandekar, J. (1992). *Biochim. Biophys. Acta*, **1120**, 123–143.
- Caine, S., Heraud, P., Tobin, M. J., McNaughton, D. & Bernard, C. C. A. (2012). *NeuroImage*, **59**, 3624–3640.
- Chamcheu, J. C., Navsaria, H., Pihl-Lundin, I., Liovic, M., Vahlquist, A. & Törmä, H. (2011). *J. Investig. Dermatol.* **131**, 1684–1691.
- Dunbar, R. C., Steill, J. D. & Oomens, J. (2011). *J. Am. Chem. Soc.* **133**, 1212–1215.
- Edwards, G. S. & Hutson, M. S. (2003). *J. Synchrotron Rad.* **10**, 354–357.
- Hutson, M. S., Hauger, S. A. & Edwards, G. (2002). *Phys. Rev. E*, **65**, 061906.
- Irvine, A. D. & Mclean, W. H. (1999). *Br. J. Dermatol.* **140**, 815–828.
- Kawasaki, T., Fujioka, J., Imai, T., Torigoe, K. & Tsukiyama, K. (2014). *Lasers Med. Sci.* **29**, 1701–1707.
- Kawasaki, T., Fujioka, J., Imai, T. & Tsukiyama, K. (2012). *Protein J.* **31**, 710–716.
- Manstein, D., Herron, G. S., Sink, R. K., Tanner, H. & Anderson, R. R. (2004). *Lasers Surg. Med.* **34**, 426–438.
- Marchuk, D., McCrohon, S. & Fuchs, E. (1985). *Proc. Natl Acad. Sci. USA*, **82**, 1609–1613.
- Miyamoto, Y., Majima, T., Arai, S., Katsumata, K., Akagi, H., Maeda, A., Hata, H., Kuramochi, K., Kato, Y. & Tsukiyama, K. (2011). *Nucl. Instrum. Methods Phys. Res. B*, **269**, 180–184.
- Morel, B., Varela, L. & Conejero-Lara, F. (2010). *J. Phys. Chem. B*, **114**, 4010–4019.
- Nomaru, K., Kawai, M., Yokoyama, M., Oda, F., Nakayama, A., Koike, H. & Kuroda, H. (2000). *Nucl. Instrum. Methods Phys. Res. A*, **445**, 379–383.
- Sipe, J. D., Benson, M. D., Buxbaum, J. N., Ikeda, S., Merlini, G., Saraiva, M. J. M. & Westermark, P. (2014). *Amyloid*, **21**, 221–224.
- Xiao, Y., Guo, M., Zhang, P., Shanmugam, G., Polavarapu, P. L. & Hutson, M. S. (2008). *Biophys. J.* **94**, 1359–1366.
- Yaji, T., Yamamoto, Y., Ohta, T. & Kimura, S. (2008). *Infrared Phys. Technol.* **51**, 397–399.
- Yamada, T., Miyoshi, N., Ogawa, T., Akao, K., Fukuda, M., Ogasawara, T., Kitagawa, Y. & Sano, K. (2002). *Clin. Cancer Res.* **8**, 2010–2014.